

https://dspace.org/

An appraisal of the pillar support system at the St. Helena gold mine

Hazell, A. A.

2015-01-26
http://hdl.handle.net/10539/16748

Downloaded from a DSpace repository. https://dspace.org/

(b) A uniformly loaded beam in cantilever is shown in FIG. 8(b).

The maximum shear stress = $\frac{3Lq}{2t}$ ..... 3.

The maximum tensile stress = $\frac{3qL^2}{t^2}$ ..... 4.

(c) A simply supported beam is shown in FIG. 8(c)

The maximum shear stress = $\frac{3qL}{4t}$ ..... 5.

The maximum tensile stress = $\frac{3qL^2}{4t}$ ..... 6.

In the equations above, the intensity of loading 'q' is initially taken to be the overburden stress in lb./in.^{2} at the depth below surface being considered. The thickness of the beam 't' from observations made underground can be taken to be 5 ft. Substituting these values into the equations above for a uniformly loaded "built-in" beam, the maximum span before fracture occurs at a load equivalent to 1,000 ft. depth, is shown to be 10 ft. Failure of the beam occurs due to excessive tensile stresses in bending. At a loading equivalent to 5,000 ft. the maximum span would be 5 ft, with the same type of failure. In practice the maximum span would be greater than that shown above since the bending beam would allow bed separation and a change of the loading condition.

Assuming a smaller uniform load of say 10 lb./in.^{2}, then a built-in beam 100 ft. in length would form before tensile failure occurred. In practice, premature failure of the beam is likely to occur at incipient fractures caused by blasting. Failure of a thin beam is not likely to result in a serious fall, but it does remove the restraint from the beam or rock mass above, and allows fracturing to continue. Initial matpack setting loads are insufficient to maintain "built-in" beams, and matpacks may carry a beam by "simple support" only.

3.2 Rock in its fractured form:

Fracture initiation occurs at micro-cracks within the grain

boundaries / .....

boundaries of the rock. These cracks may propogate depending on the stress conditions and failure may occur producing the shapes and sizes of rocks commonly observed underground. A knowledge of the behaviour of the fractured zone which surrounds the excavation is extremely important, since the stability of this zone determines the safety of the mining operation.

Rock fracture has been demonstrated by A.A. Griffiths and others, to initiate in favourably orientated minute cracks or pores in the rock. It can be shown that a concentrated tensile stress field exists at the tip of such a crack and if this stress is greater than the molecular cohesion of the rock, further cracking will result. If the assumption is made that microcracks or pores are elliptical in shape, then the tensile stress applied to the model (σ_a) necessary to cause rock fracture is given by :-

$$\sigma_a = \sqrt{\frac{Y E}{2C}} \qquad \ldots\ldots\ldots\ldots 7.$$

Y is the specific surface energy of the material
(6×10^{-4} lb. in. / in.^{2})
(for hard rock).

E is Young's Modulus

C is the length of the crack

A tensile stress field exists at the tip of a microcrack when the applied stress normal to the crack is tensile. In a compressive field, however, the crack may be initially closed and the frictional forces which occur due to the contact between the crack faces must be overcome before the crack can extend. There are therefore, two stress criteria for crack propogation depending on whether the crack is initially closed or open. FIG. 9 shows the relationship between the critical crack orientation and the principal stress ratio.

Hoek has concluded from tests made on various materials[3] that failure of a specimen cannot occur as a result of a single crack in the material, except in a tensile stress field. In a compressive field the presence of a favourable array of cracks is essential for

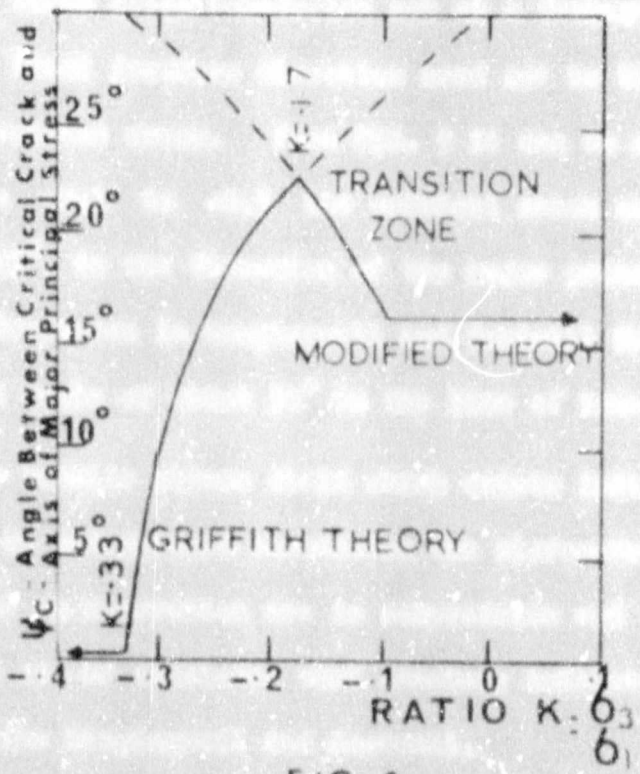


FIG 9

The Relationship Between the Critical Crack Orientation and the Principal Stress Ratio

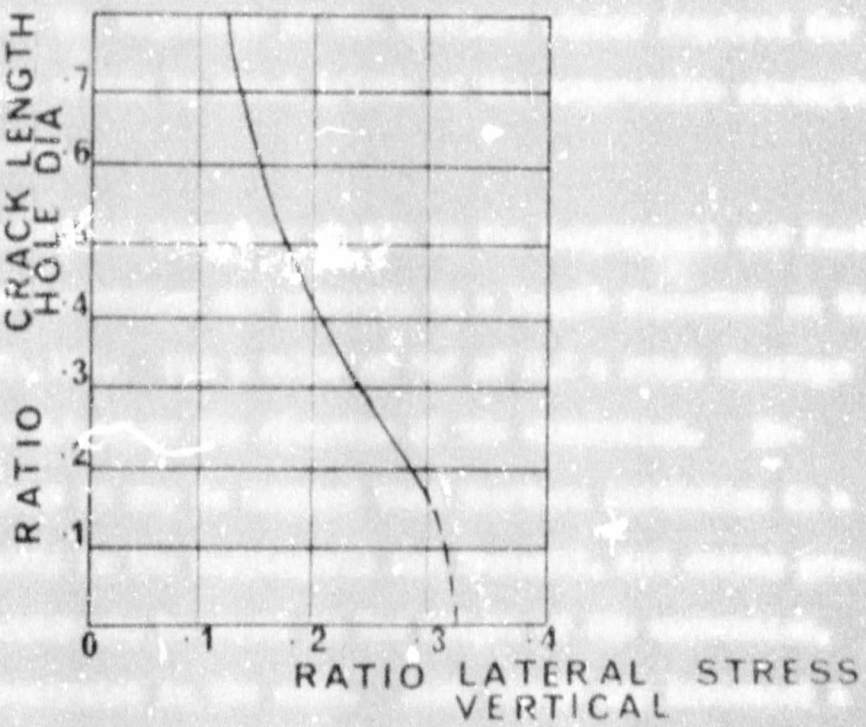


FIG 10

Tensile Crack Development at the Top and Bottom of a Circular Hole

rock fracture on a macro scale. Photographic evidence shows that the crack propogates along grain boundaries of a specimen under uniaxial compression. These grain boundaries act as a favourable array of cracks and the final fracture direction need not be that of the most favourably orientated crack. From FIG. 9 it can be seen that for values of k = -0.1 to -0.3 the critical crack orientation lies between 0 and 23°, to the direction of the major principal stress. However, rock fractures in hangingwall and footwall in certain stopes show a constant angle of about 30° to the line of true dip.

In the tensile stress field which exists initially in the hangingwall of an underground excavation the micro-cracks must be open. The sidewalls of an excavation are in compression and the cracks will be closed. It can be concluded that fracture initiation is more likely to commence in the hangingwall and footwall.

A study of fracture development around a circular hole cut in a rock plate model and subjected to a bi-axial stress field has been made by Hoek[3]. This study revealed that fracture initiation and propogation occurs in regions in which the minor principal stress is zero or tensile and that the magnitude of the vertical stress required for propogation of such cracks is about 1/10th of the compressive strength of the model material.

Crack initiation therefore starts in the hangingwall and footwall of a circular excavation and proceeds to a length dependant on the value of 'k', (FIG. 10). For a value of 'k' of 0.2 a crack develops equal in length to 0.4 times the diameter of the excavation. Extending this argument it may be assumed that fracture initiation in a drive or raise starts in the hangingwall and footwall, and cracks proceed to a length which may be equal to the height of the excavation, depending on the restraint in the rock. Such cracks may intersect a plane of weakness and assist the formation of the fracture zone.

As the stoping excavation increases, the vertical extent of the tensile zone in the hangingwall also increases and, therefore,

separation / .....

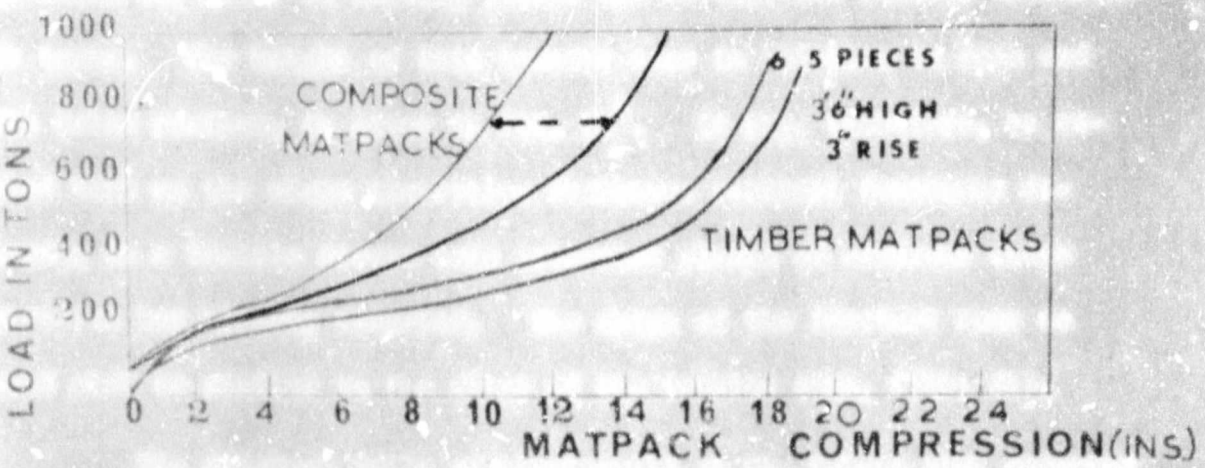


FIG 11

Matpack Characteristics

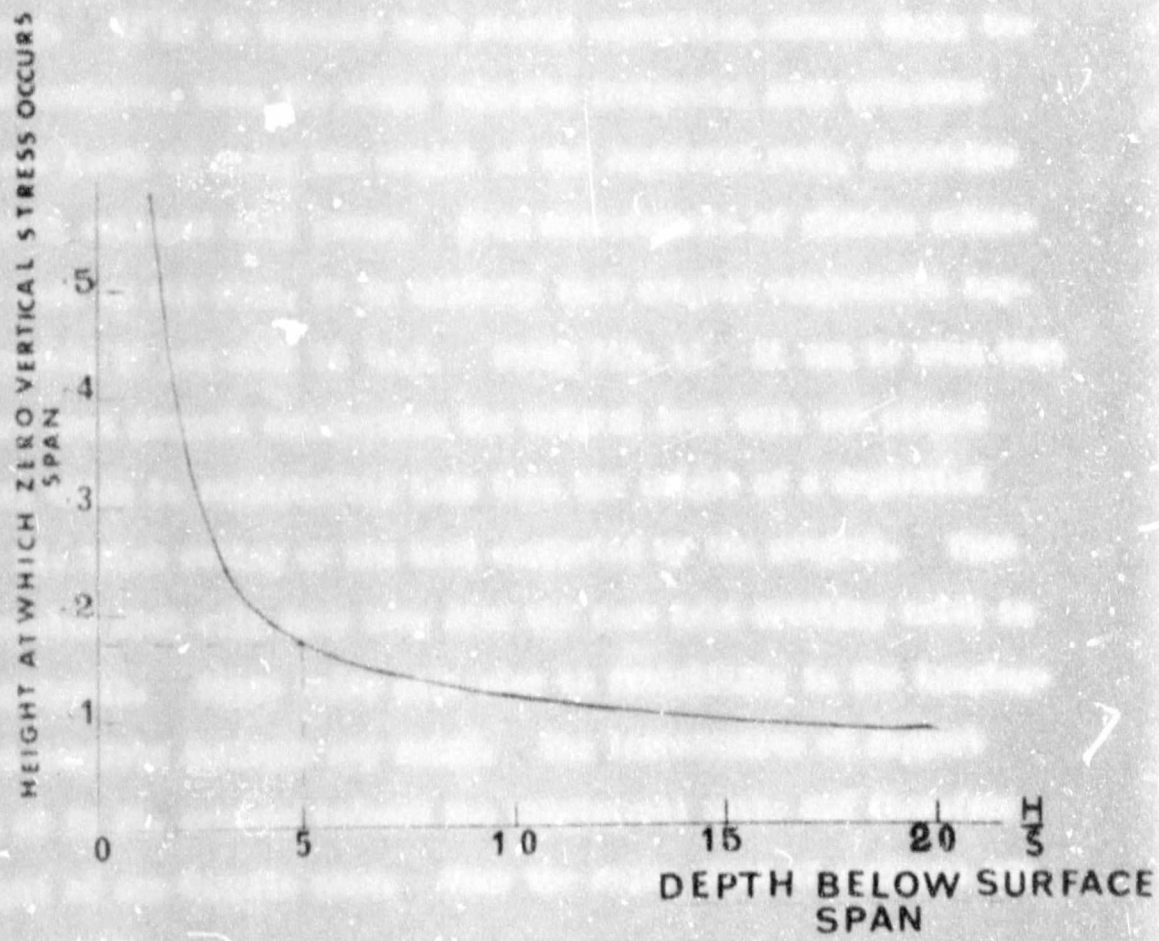


FIG 12

separation may occur at bedding planes and at contacts between different rock types. The height of this tensile zone in relation to span and depth below surface, is given in FIG. 12[4]. It may, therefore, be expected that as the stope excavation increases vertical fractures developing in a tensile stress zone intersect planes of weakness where separation has already occurred. The shape of the fracture zone so formed must be similar to the shape of the tensile zone, (FIG. 21).

The original falls of hangingwall on St. Helena Mine occurred at spans between 200 and 400 ft. in stopes which were at a depth of 1,000 ft. Expressing these figures as a ratio of depth to span, FIG. 12 can be used to indicate a plane of weakness in the hangingwall of the stopes. The two ratios are 5 and 2.5 respectively, and the heights at which the tensile region intercepts a plane of weakness are calculated from FIG. 12 as 34 ft (.16 x 200), and 100 ft. (.24 x 400), respectively. If it is assumed that strata separation occurs along the plane of weakness, then the stope supports (matpacks) must generate sufficient loads to carry the weight of the separated rock, otherwise hangingwall collapse will occur. From measurements of closure subsequently made on the mine, it is unlikely that matpack compression anywhere exceeds 18 per cent (6 in.). Using FIG. 11[8] it can be seen that at 18 per cent matpack compression the matpack load will not exceed 260 tons, which is considerably less than the weight of a separated slab 34 ft. thick acting on the area supported by the matpack. Thus the separated slab will drop away from the rock mass creating voids in the hangingwall. These voids give rise to instability in the hangingwall and complete collapse may occur. The introduction of support pillars at 90 ft. centres reduced the hangingwall spans and therefore the height of the tensile zone. Thus the major plane of weakness was not intercepted.

Observations show that in the majority of cases the hangingwall blocks stabilize themselves. The stability of such a mass of rock can be explained by considering that the internal forces form an 'arch' between abutments[5]. The theory of the Voussoir Arch assumes

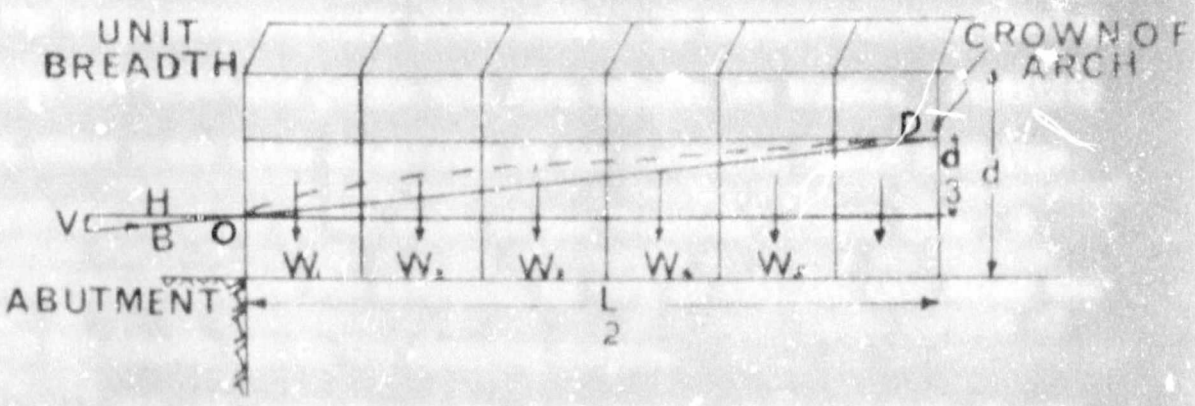


FIG 13

Stability of the Horizontal Voussoir Arch

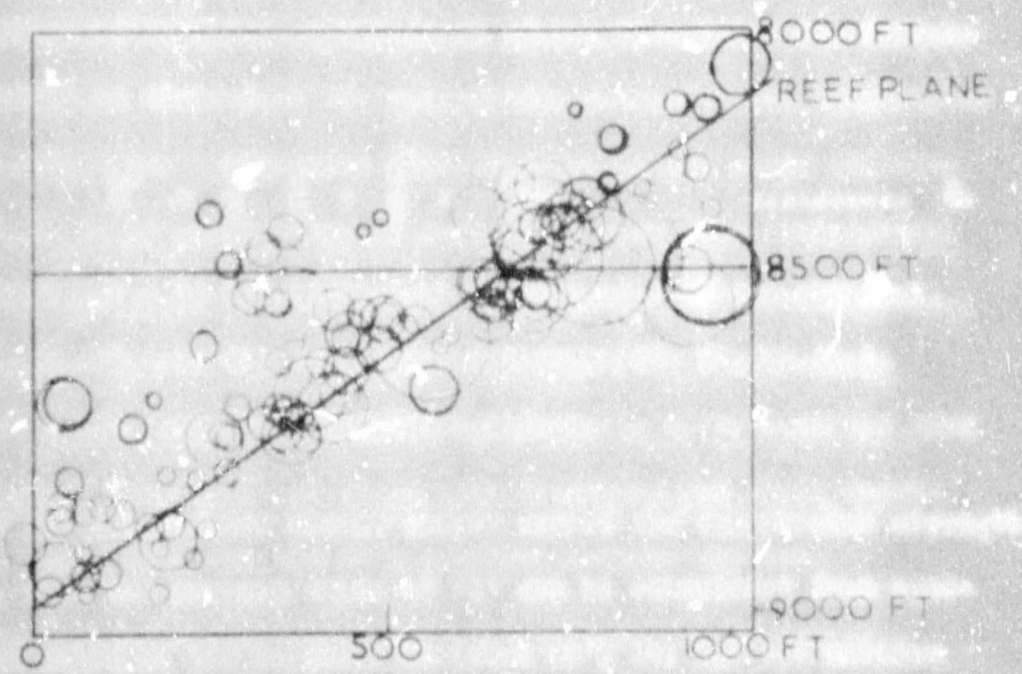


FIG 14

Foci of Seismic Events around a Stope Excavation

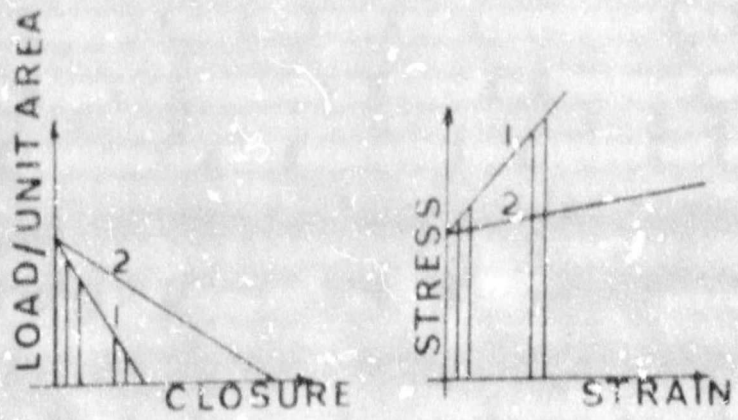


FIG 15

Load Closure Graph for the Stope hanging wall

Strain Energy Change Ahead of the Stope Face

that an arch is stable if all the stresses remain compressive and within the compressive strength of the rock. If tensile stresses develop within the 'arch' pin joints will form between the blocks. Stability will occur under these conditions if the equivalent linear arch lies in the middle third of the depth of the "Voussoir", (FIG. 13). A further consideration for stability is that no slipping must occur between the blocks due to the shearing forces.

FIG. 13 shows the stable arch formed of "Voussoirs" of unit breadth and of varying weights. The dotted line "OD" is a true parabolic arch and the straight line "OD" is the approximate equivalent linear arch. The depth of each "Voussoir" or block is represented by "d" and the length of the span by "L". If the equivalent linear arch lies within the middle third of the depth of the "Voussoir" the following relationship is derived:-

$$L^2 = \frac{4}{3}\,\frac{H}{D} = \frac{4}{3} \times \frac{d\sigma}{D} \qquad \ldots\ldots\ldots\ 8.$$

Where H is the horizontal force acting at the abutment.

D is the density of the rock (170 lb./cu.ft.).

σ is the compressive stress.

If the compressive stress cannot exceed the compressive strength of the rock, then the maximum value of 'L' can be calculated from equation 8. The depth of the Voussoir is taken as 5 ft. and the maximum stress as 30,000 lb./in.^{2} Therefore the maximum span that can occur between solid abutments is 420 ft.

If it is assumed that the rock mass surrounding the excavation is fractured, then the abutment is formed of fractured material. In this case the equations of soil mechanics are applied and equation 8 becomes :-

$$L = 1.15\ (\tan 45^\circ - \tfrac{\phi}{2}) \sqrt{\int I\,dz} \qquad \ldots\ldots\ldots\ 9.$$

Where I is the vertical abutment loading index i.e., the ratio of the vertical stress in the abutment to the overburden stress.

z is / .....

z is the depth from the surface.

Ø is the internal friction angle of the rock.

d is the depth of Voussoir

Substituting into equation 9 a loading index of 4, an internal fracture angle of 50° and a depth of Voussoir of 5 ft., the maximum value of 'L' is calculated to be 125 ft. at a depth below surface of 5,000 ft.

It can be seen from the results obtained above that a solid pillar can support a Voussoir arch of greater span than a fractured pillar. As the depth below surface increases and pillars become more fractured they will carry less of the hangingwall loads.

The fracture of the hangingwall into blocks does not continue indefinitely and is limited by the restraining forces on the boundary of the elastic rock mass. Practical determination of the shape and size of this zone is being carried out at present at East Rand Proprietary Mines, Limited and at Harmony Gold Mine by using seismic techniques. Any sudden disturbance of the equilibrium stresses in a rock mass, (i.e., violent rock fracture), causes seismic waves to be radiated from the disturbance. The foci of these rock fractures and their magnitudes can be found with the aid of a suitable seismic network.

FIG. 14 shows the location of the seismic events around a stope excavation[7]. The centre of a circle represents the centre of a disturbance, and the diameter the magnitude of the disturbance. By implication, FIG. 14, shows the approximate shape and size of the fracture zone. The height of this fracture zone is equal to the height of the tensile zone, as obtained from FIG. 12 for the same stope span and depth below surface. It is therefore possible that FIG. 12 can be used to estimate the height of the fracture zone.

FIG. 14 shows that the fracture zone takes the form of a very flat ellipse. Theoretical calculations also show that the fracture zone is elliptical in shape[2]. The results of tests on Harmony Mine show that the existance of weak layers of shale have influenced

the / .....

the positions of the foci of the seismic events. It may be assumed that the shale bands in the hangingwall on St. Helena will have a similar effect.

The size of the fracture zone is influenced by the strength and characteristics of the stope support. The abutment forces of the Voussoir Arches formed at the matpacks, stone walls and internal stope pillars may be resolved into component forces acting at the boundary of the fracture zone. The effect of these forces is to form a biaxial stress field at the boundary and so prevent further fracturing[2].

3.3 Energy Relationships:

Rock bursts may be defined as damage to underground workings caused by the uncontrolled disruption of rock associated with a violent release of energy. Cook and others[6] have shown that energy relationships can be used to estimate the rock burst hazard.

The mining of an excavation allows the lowering of the rock mass above it and hence a loss of potential energy (W_G). If the rock mass is elastic, half of this potential energy is stored as strain energy (W_S) in the solid rock ahead of the stope face and the other half is released (W_R) into the excavation. This relationship is given by :-

$$\frac{W_G}{2} = W_S = W_R \qquad \ldots\ldots\ldots\ldots \quad 10.$$

FIG. 15B shows the relationship between stress and strain ahead of the stope face and the stored energy is equal to half the stress multiplied by the strain. The energy released is shown in FIG. 15A as the area under the stress closure curve for the stope hangingwall. It can be seen that the majority of the energy is released in the initial stages of closure. The energy released for a horizontal excavation, which is long compared with its span, is given by the equation[6 & 7] :-

$$E = \frac{4P^2 \ S^2}{3G} \qquad \ldots\ldots\ldots\ldots \quad 11.$$

In / .....

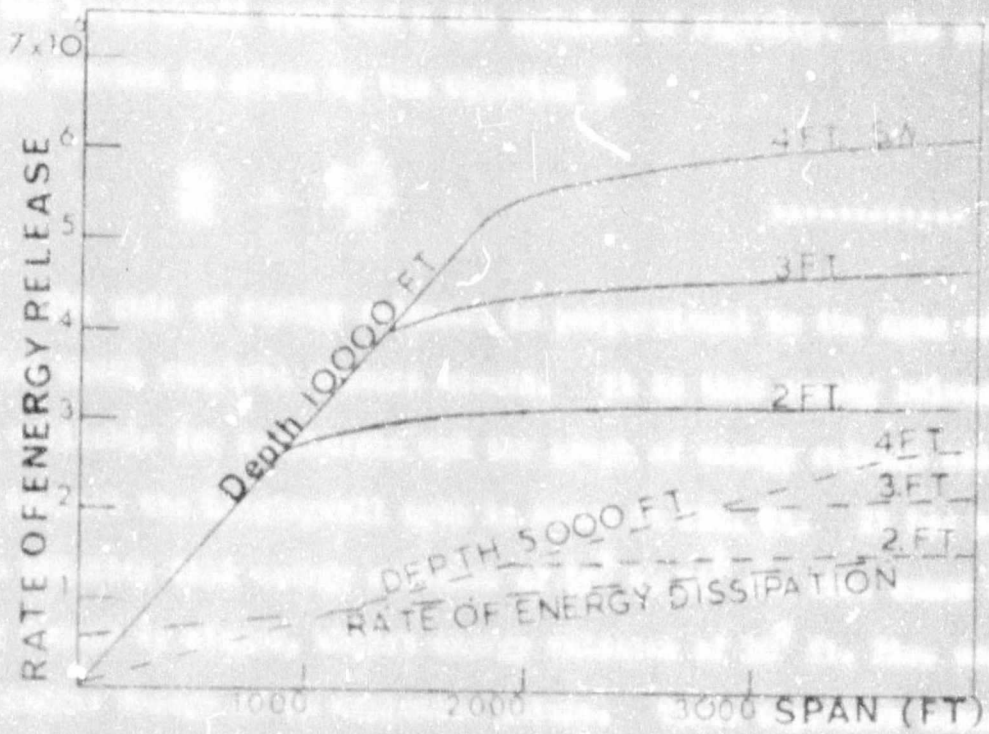


FIG 16

Relationship between Rate of Energy Release and Stope Span

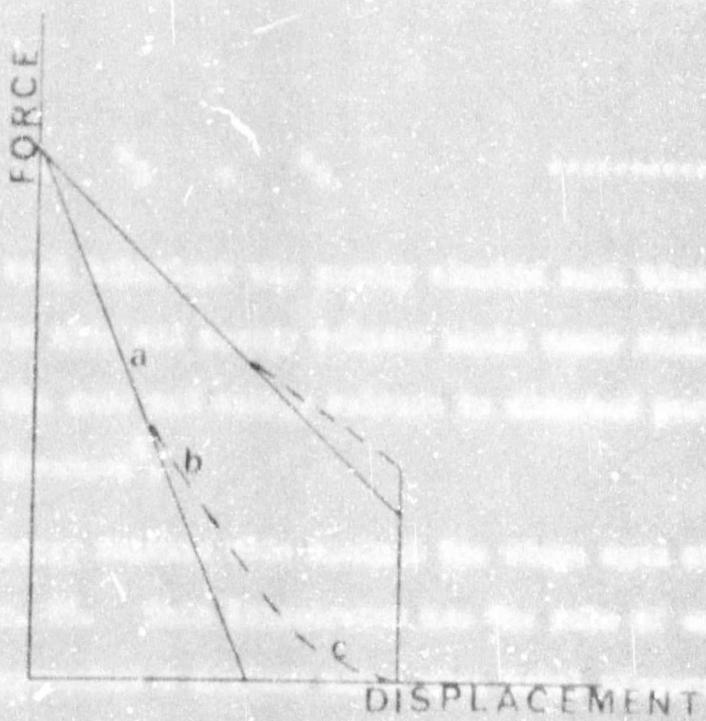


FIG 17

Modified Force Displacement Diagram

for the Stope Hangingwall

In this equation the term P represents the virgin stress, S half the hangingwall span and G the modulus of rigidity. The rate of energy release is given by the equation :-

$$\frac{dE}{dS} = \frac{8P^2S}{3G} \qquad \ldots\ldots\ldots\ldots \quad 12.$$

The rate of energy released is porportional to the span of excavation until complete closure occurs. It is this energy released that is available for rockbursts and the graph of energy release rate plotted against the hangingwall span is shown in FIG. 16. It has been found in practice that energy releases of 10^5 to 10^8 ft. lbs. cause increasing damage to stopes, whilst energy releases of 10^9 ft. lbs. cause very extensive damage of an explosive nature. These explosive occurrences are commonly referred to as rock bursts. Now the effect of rock fracture is to increase closure and therefore the amount of energy released and the force displacement diagram as shown in FIG. 15A is modified as shown by FIG. 17. The diagram comprises an elastic part (a) a non-linear deviation at the onset of fracture (b) and a non-linear deviation associated with bed separation (c). The energy relationships now become :-

$$\frac{W_G}{2} = W_S \leq W_R \qquad \ldots\ldots\ldots\ldots \quad 13.$$

Now if the rock behaviour was purely elastic each blast would increase the excavation size and energy release would occur violently. However, this is not the case and energy release is absorbed partly by the increase in rock fracture[6].

A plot of energy release rate against the stope span at two depths is shown in FIG. 16. This illustrates how the rate of energy release changes and approaches a maximum value when total closure of hangingwall and footwall occurs. This maximum value is equal to the product of the stoping width and the overburden stress, and therefore the rock burst hazard is less in stopes of lower stoping width. The effect of lower stoping width can be achieved by effective stope support.

This / .....

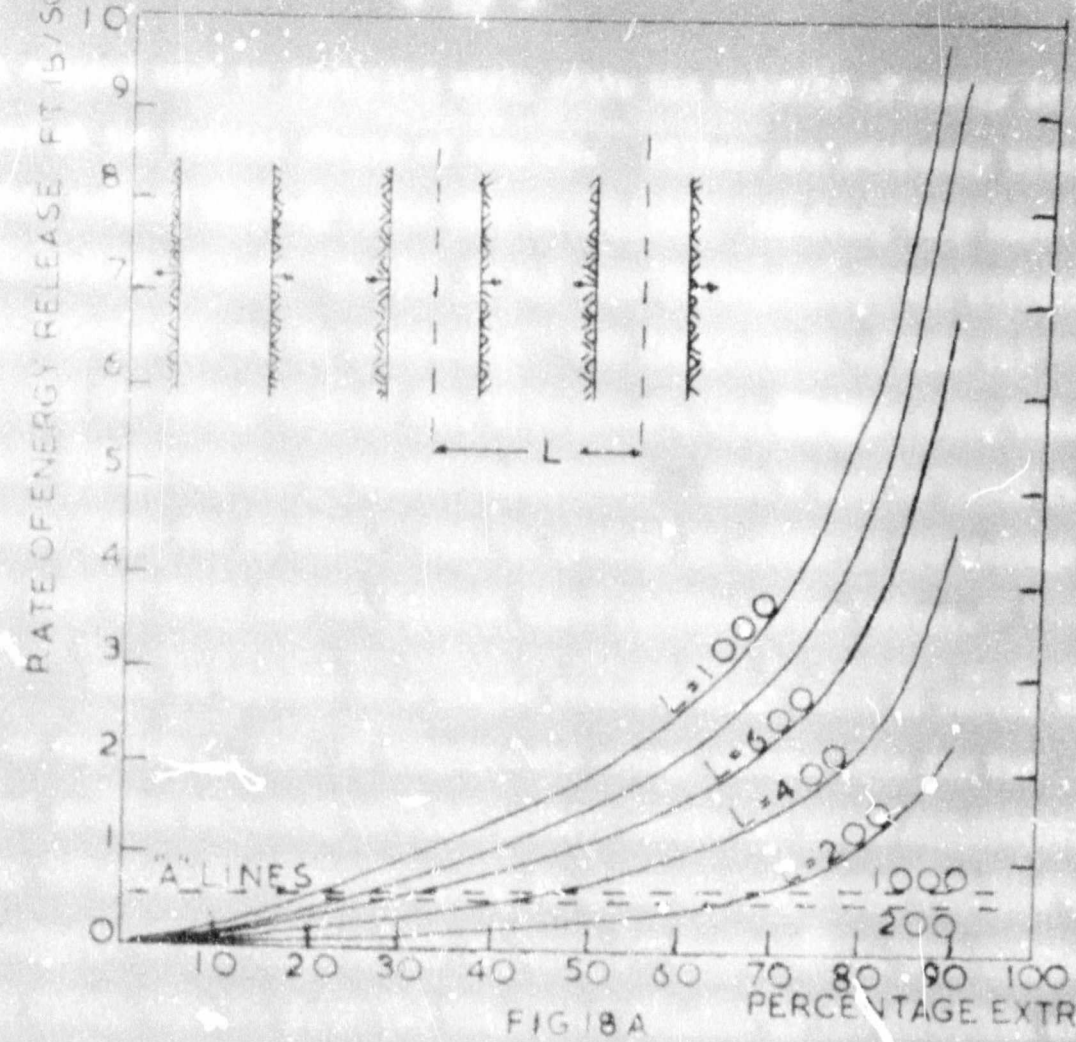


FIG 18A

RATE OF ENERGY RELEASED BY PARALLEL LONGWALL FACES IN A DIRECTION PERPENDICULAR TO THEIR LONG AXES

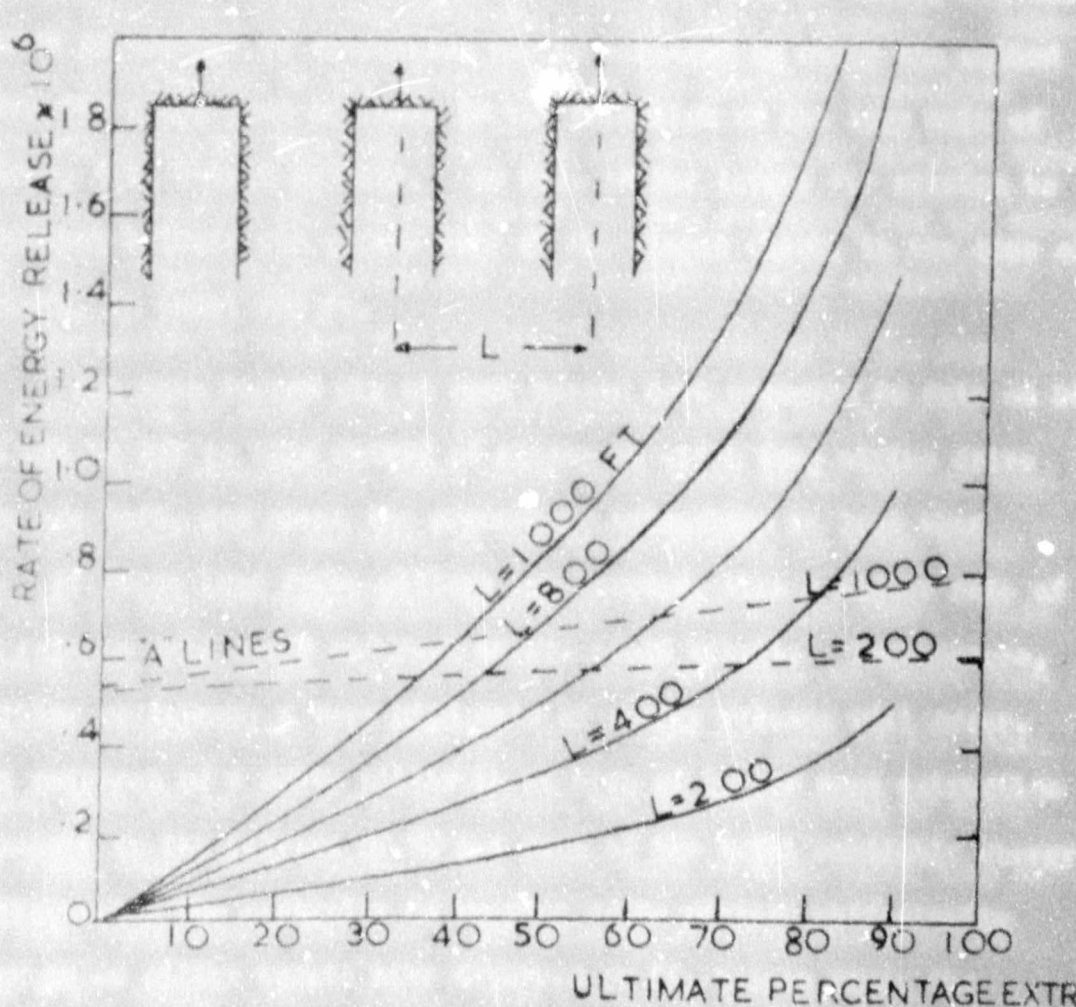


FIG 18B

RATE OF ENERGY RELEASED BY PARALLEL STOPES FACES ADVANCING IN DIRECTION OF LONG AXES OF PANELS

This support must be installed early since the majority of energy is released at the initial stages of closure. Pillars are obviously better in this respect than any other form of support. However, they must not be removed later. In FIG. 16 the line (A) represents the effective energy absorption due to fracturing. The intersection of this (A) line with the energy release rate line gives a typical span below which violent energy release is almost impossible. Such a span at 5,000 ft. is about 1,000 ft. in size. This is greatly in excess of the average stope span of about 600 ft. between drive pillars on St. Helena.

FIG. 16 applies to a single isolated stope which is rarely the case on any mine. FIG. 18 compares the energy release rate for two general methods of mining in which several stopes are mined concurrently. Method 'a' shows the longwall system in which the stope face advances at right-angles to the long axis of the stope. Method 'b' is that adopted on St. Helena Mine in which the stope face advances in the direction of the long axis of the stope. The rate of energy release plotted against percentage extraction is shown for the two methods at a depth of 10,000 ft. A comparison illustrates that for the same rate of energy release a greater percentage of extraction can be achieved by using the method in which the stope face advances in the direction of the long axis of the stope, (St. Helena method). In FIG. 18 the letter 'L' relates to the distance between the centre line of the stopes which, in the case of St. Helena, is about 800 ft.

The main reason why no rock bursts have occurred to date on St. Helena may be due to this method of mining in which long strike drive pillars are left, and where the percentage extraction is less than fifty. If these long drive pillars are removed, than a higher rate of energy release will occur and rock bursts could result. Furthermore, if a pillar collapses, a very high rate of energy release will occur. A total collapse of a drive pillar in an area of 50 per cent extraction would result in the release of 80 per cent of the total available energy[7]. This illustrates the necessity of keeping drive pillars sufficiently wide and as no pillar bursts have occurred on St. Helena Mine, the pillar width appears to be adequate at a depth of 5,000 ft.

4. CHARACTERISTICS OF MINE SUPPORTS

It is known that an underground excavation is surrounded by a fracture zone, but outside this zone it is assumed that the rock mass is solid and elastic. As a stope excavation increases the fracture zone increases in size, and it is the stability of this fracture zone that must be maintained by normal stope supports. The more effective the support system the smaller may be the size of the fracture zone, since greater restraining forces occur at the boundary of the zone. At depths of 5,000 ft. and greater the method of mining must be designed to minimise the rock burst incidence.

The types of support used in stopes on St. Helena are pillars, timber matpacks and stonewalls. It is proposed in this section to discuss the characteristics of each of these types of support from general observations made on St. Helena and from tests carried out on other mines.

4.1 Matpacks:

There are few recorded tests on this type of support. Tests have been carried out in the laboratory[8] by the National Mechanical Engineering Research Institute, and from the many results obtained those applying to a typical St. Helena chock have been selected, and are shown in FIG. 11. This figure shows the load in tons plotted against the chock compression in inches for a 2 ft. 8 ins square by 36 ins high chock consisting of mats of five or six pieces with 3 ins to 4 ins rise. The load compression curve shows that there is an initial convex portion, due to the settling of the chock pieces, in which about 6 per cent (2 ins) of compression occurs at a load of 150 tons. This is followed by a straight portion of the curve in which the chock compression increases to 40 per cent (14 ins) and the load to 350 tons. The final portion of the curve is concave due to the meeting of chock pieces along their full length. The final load reaches 1,000 tons at 50 per cent compression (18 ins) The maximum setting load obtained with an 8 lb. hammer was 11 tons. The effect of stoping width on the

matpack / .....

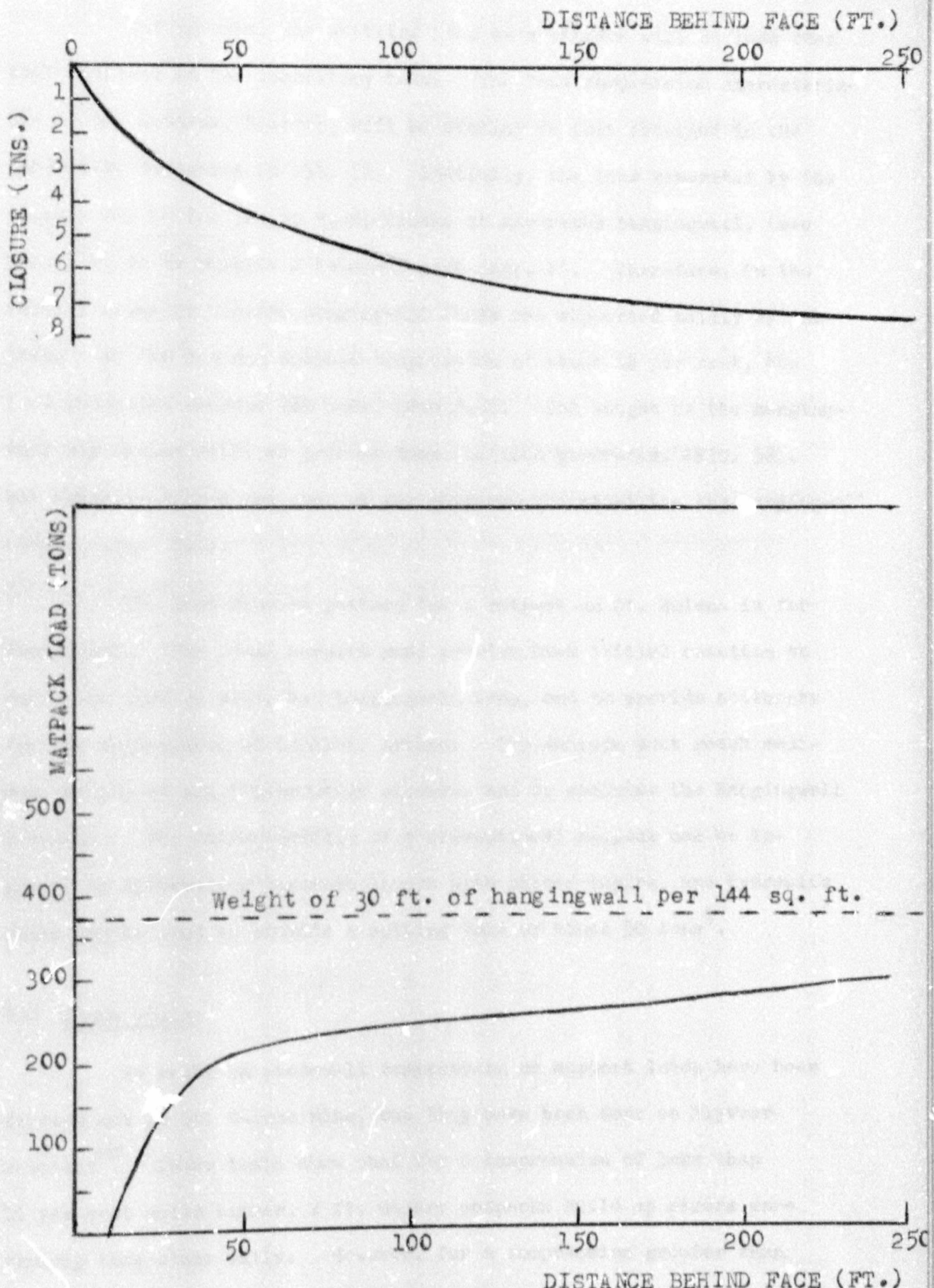


FIG. 52

A comparison of the load generated by a matpack with the load necessary to hold 30 feet of hangingwall.

matpack characteristic is important. The lower the stoping width the greater the percentage compression of the matpack, and therefore the higher the matpack resistance for the same closure.

Underground, the settling load on a matpack will be less than that achieved in the laboratory test. The load compression characteristic of the matpack, however, will be similar to that obtained in the laboratory and shown in FIG. 11. Initially, the load generated by the matpack may be too low to carry blocks of separated hangingwall, (see FIG. 52), or to support a Voussoir Arch (App. V). Therefore, in the initial stage of closure hangingwall loads are supported mainly by pillars. At the maximum matpack compression of about 18 per cent, the load generated reaches 260 tons, (Sec.3.2). The weight of the hangingwall blocks may still be greater than the load generated, (FIG. 52), but Voussoir Arches may abut at the matpacks and stabilize the hangingwall blocks, (Sec. 3.2).

The load closure pattern for a matpack on St. Helena is far from ideal. The ideal support must provide high initial reaction to carry the load of separated hangingwall beds, and to provide abutments for the development of Voussoir Arches. The matpack must reach maximum loading at small percentage closure, and so minimise the hangingwall movement. The characteristic of a conventional matpack can be improved by alternating concrete layers with timber layers, and hydraulic jacks can be used to provide a setting load of about 50 tons[9].

4.2 Stone Walls:

No tests on stonewall compression or support loads have been carried out on St. Helena Mine, but they have been done on Blyvooruitzicht[10]. These tests show that for a compression of less than 15 per cent solid timber, 2 ft. square matpacks build up stress more rapidly than stone walls. However, for a compression greater than 15 per cent, the reverse was true. Now the percentage closure on St. Helena up to the stage of drive pillar extraction is less than 15 per cent. Therefore matpacks may provide a better support up to

this / .....

Author Hazel AA
Name of thesis An appraisal of the pillar support system at the St Helena gold mine. 1968

PUBLISHER:
University of the Witwatersrand, Johannesburg
©2013

LEGAL NOTICES:

Copyright Notice: All materials on the University of the Witwatersrand, Johannesburg Library website are protected by South African copyright law and may not be distributed, transmitted, displayed, or otherwise published in any format, without the prior written permission of the copyright owner.

Disclaimer and Terms of Use: Provided that you maintain all copyright and other notices contained therein, you may download material (one machine readable copy and one print copy per page) for your personal and/or educational non-commercial use only.

The University of the Witwatersrand, Johannesburg, is not responsible for any errors or omissions and excludes any and all liability for any errors in or omissions from the information on the Library website.